Asociación Argentina
de Mecánica Computacional

Mecánica Computacional Vol XXXI, págs. 4143-4152
Alberto Cardona, Paul H. Kohan, Ricardo D. Quinteros, Mario A. Storti (Eds.)
Salta, Argentina, 13-16 Noviembre 2012

THERMAL COUPLING IN PARTICLE FINITE ELEMENT METHOD - SECOND GENERATION

Diego M. Sklar[a], Juan M. Gimenez[b], Norberto M. Nigro[a,b] and Sergio Idelsohn[a,b,c]

[a]*Facultad de Ingeniería y Ciencias Hídricas - Universidad Nacional del Litoral. Ciudad Universitaria. Paraje "El Pozo", Santa Fe, Argentina, http://www.fich.unl.edu.ar*

[b]*International Center for Computational Methods in Engineering (CIMEC), INTEC-UNL/CONICET, Guemes 3450, Santa Fe, Argentina, http://www.cimec.org.ar*

[c]*ICREA Research Professor at the International Center for Numerical Methods in Engineering (CIMNE), Edificio C1, Campus Norte UPC C/ Gran Capitán S/N 08034 Barcelona, España, http://www.cimne.edu.es/*

Keywords: PFEM-2, particles, CFD, parallel computing, Boussinesq approximation, buoyancy term.

Abstract. In previous papers (Idelsohn et al., 2012) the numerical method called Particle Finite Element Method - Second Generation (PFEM-2) was presented. It solves scalar and vectorial transport phenomena such as Navier Stokes equations for transient, laminar and incompressible flows. This method is characterized by a Lagrangian formulation that uses both particles and mesh to solve physics equations. Taking advantage of that, particles can transport physics variables that any model includes, this paper presents an evolution of the method for solving equations that govern the fluid flow coupled with passive-scalar transport equations, such as species concentrations or temperature. Also, the explicit streamline integration strategy used by the method allows to update each variable following its own physic law in an efficient way. This paper places particular emphasis in the thermal coupling through a buoyancy term added to fluid acceleration and transporting at each particle its temperature. Regarding to the implementation, it follows the parallel computing strategy presented above. Finally, results obtained in typical benchmark cases, such as thermal square and cubic cavity, are presented, comparing with bibliographic and experimental data.

1 REVIEW OF PFEM-2 METHOD

The goal of PFEM-2 is to solve transport-equations. The method is principally motivated for solving viscous incompressible flow equations as fast as possible. Its formulation allows to find numerical results of others scalar or vectorial transport equations, such as energy balance equation, turbulence modeling, species transport and also, the coupling among them.

The Lagrangian expression for a scalar transport-equation is

$$\frac{D\phi}{Dt} = \nabla \cdot (\alpha \, \nabla\phi) + Q. \tag{1}$$

where the unknown is the scalar ϕ (if ϕ is the temperature, this equation is called *Heat Equation*, where α is the thermal diffusivity), and Q is an external source.

On the other hand, *Navier-Stokes* equation system describes the behavior of newtonian viscous incompressible fluid flow. Its formulation is based on momentum-transport equation which is normally coupled with the equation for the local mass balance. The Lagrangian expression is:

$$\rho\frac{D\mathbf{v}}{Dt} = -\nabla p + \mu(\nabla\mathbf{v}^T + \nabla\mathbf{v}) + \mathbf{Q}, \tag{2}$$

$$\nabla \cdot \mathbf{v} = 0. \tag{3}$$

where the unknowns are the velocity vector $\mathbf{v}$ and the pressure p, and ρ is the density and μ the dynamic viscosity.

It should be noted that the left terms in equations (1-2) include a material derivative instead of a temporal derivative plus a convective term (equation 4) like is usual in Eulerian formulation.

$$\frac{D\phi}{Dt} = \frac{\partial\phi}{\partial t} + \mathbf{v} \cdot \nabla\phi. \tag{4}$$

Lagrangian formulation is used to simplify some calculations (especially the non-linear convective term in momentum equation) normally found in Eulerian formulation and specially because its natural adaptation for particle based methods.

It is well known that the time step selected in the solution of the transport equations is stable only for time steps smaller than two critical values: the Courant-Friedrichs-Lewy (Co) number and the Fourier (Fo) number (Donea and Huerta, 2003). The first one concerns with the convective terms and the second one with the diffusive ones. In Eulerian formulation both numbers must be less than a constant value close to one to have stable algorithms. For convection dominant problems like high Reynolds number flows, the condition $Co < 1$ becomes crucial and limits the use of explicit methods or makes the solution scheme far from being efficient.

However, the key of the PFEM-2 algorithm(Idelsohn et al., 2011) is the ability to reach $Co \gg 1$ due to the information is transported on the particles. One of the novelty in PFEM-2 respect to its predecessor PFEM concerns with the integration of particle trajectory and the state variables defining the problem. This integration is performed following the streamlines computed explicitly with the information of the previous time step. This new method was named X-IVAS method (eXplicit Integration following the Velocity and Acceleration Streamlines). It was presented in Idelsohn et al. (2012) and it represents a more stable explicit time integration not limited by Co. Briefly, the algorithm takes the velocity field as stationary on each time step ($\mathbf{v}^n$), then the particle position follows these streamlines and the particle state variables are updated by the change rate determined by the physics equations.

$$\mathbf{x}_p^{n+1} = \mathbf{x}_p^n + \int_0^{\Delta t} \mathbf{v}^n(\mathbf{x}_p^\tau)\, d\tau \tag{5}$$

$$\phi_p^{n+1} = \phi_p^n + \int_0^{\Delta t} \mathbf{g}^n(\mathbf{x}_p^{n+\tau}) + Q^{n+\tau}\, d\tau \tag{6}$$

$$\mathbf{v}_p^{n+1} = \mathbf{v}_p^n + \int_0^{\Delta t} \mathbf{a}^n(\mathbf{x}_p^{n+\tau}) + \mathbf{f}^{n+\tau}\, d\tau \tag{7}$$

where $\mathbf{a}^n = -\nabla p^n + \mu(\nabla \mathbf{v}^{nT} + \nabla \mathbf{v}^n)$ and $\mathbf{g}^n = \nabla \cdot (\alpha\, \nabla \phi^n)$, are nodal variables.

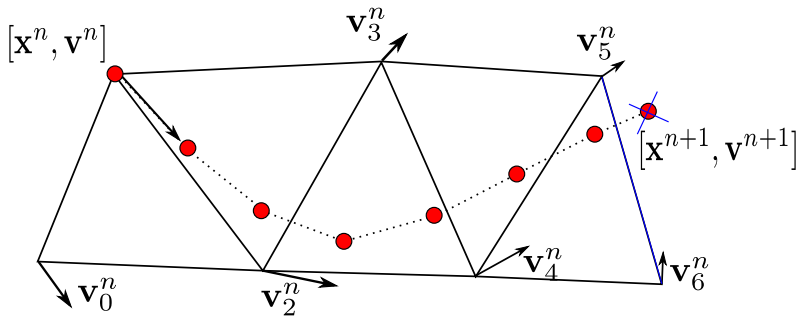

Figure 1: Streamline integration updating the particle position and state.

To solve the passive scalar transport equation with a known velocity field, the equations (5-6) must be used. After streamline integration, nodal values must be updated. If you want to transport N passive scalars with the same velocity field, you only have to solve equation 6 for each variable with a common convective transport for all the passive scalars. Thereby multi-species problems also may be simulated with PFEM-2 in a more efficient way.

To solve the Navier Stokes equation, systems (5-7) are solved coupled with the pressure p. Figure 1 shows a graphical interpretation of the streamline integration for incompressible flow problems. The fractional-step method is used to solve the coupling between the pressure and the velocity. Here, it is also necessary to update nodal states with the states transported by particles.

There are two approaches to update nodal states after streamline integration, each one generates two versions of the method. They are:

- *PFEM-2 Mobile Mesh:* Remesh the geometry with new particles position (particles↔nodes).
- *PFEM-2 Fixed Mesh:* Project states from particles to nodes, preserving the mesh.

This work is based on PFEM-2 Fixed Mesh version because it avoids the remeshing at each time-step, a very time consuming process. Even though the Mobile Mesh version was the first developed, at present it is in stand-by status while an efficient algorithm for parallelizing the remeshing is being done. The Fixed Mesh version has the advantage of no need remeshing and due to the possibility of factorizing the matrix of the pressure equation only once it becomes much more efficient. Moreover, this last feature may be extended also for the diffusion part of the equation while constant in time coefficient parameters are involved, as in laminar flow regime.

Finally, a brief review is presented in the Algorithms 1 and 2.

Algorithm 1 - Time Step PFEM-2 Scalar Transport

1. Calculate scalar change rate on the nodes like a FEM (Finite Element Method):
   $\int_\Omega \boldsymbol{N}\ \mathbf{g}^n\ d\Omega = -\int_\Omega \nabla \boldsymbol{N}\ \alpha \nabla \phi^n\ d\Omega + \int_\Gamma \boldsymbol{N}\ \nabla \phi^n \cdot \eta\ d\Gamma$
2. Evaluate new particles position and state following the streamlines:
   $\mathbf{x}_p^{n+1} = \mathbf{x}_p^n + \int_0^{\Delta t} \mathbf{v}^n(\mathbf{x}_p^\tau)\ d\tau$
   $\phi_p^{n+1} = \phi_p^n + \int_0^{\Delta t} \mathbf{g}^n(\mathbf{x}_p^{n+\tau}) + Q^{n+\tau}\ d\tau$
3. Update particles inventory
4. Project state to the mesh:
   $\phi_j^{n+1} = \boldsymbol{\pi}(\phi_p^{n+1})$

Algorithm 2 - Time Step PFEM-2 Incompressible Flow

1. Calculate acceleration on the nodes like a FEM:
   $\int_\Omega \boldsymbol{N}\ \nabla \cdot \boldsymbol{\tau}^n\ d\Omega = -\int_\Omega \nabla \boldsymbol{N} \cdot (\mu \nabla \mathbf{v}^n)\ d\Omega + \int_\Gamma \boldsymbol{N}\ \nabla \mathbf{v}^n \cdot \eta\ d\Gamma$
   $\int_\Omega \boldsymbol{N}\ \nabla p^n\ d\Omega = -\int_\Omega \nabla \boldsymbol{N}\ p^n\ d\Omega + \int_\Gamma \boldsymbol{N}\ p^n \cdot \eta\ d\Gamma$
   $\mathbf{a}^n = \nabla \cdot \sigma = -\nabla p^n + \nabla \cdot \boldsymbol{\tau}^n$
2. Evaluate new particles position and state following the streamlines:
   $\mathbf{x}_p^{n+1} = \mathbf{x}_p^n + \int_0^{\Delta t} \mathbf{v}^n(\mathbf{x}_p^\tau)\ d\tau$
   $\hat{\mathbf{v}}_p^{n+1} = \mathbf{v}_p^n + \int_0^{\Delta t} \mathbf{a}^n(\mathbf{x}_p^{n+\tau}) + \mathbf{f}^{n+\tau}\ d\tau$
3. Update particles inventory
4. Project state to the mesh:
   $\mathbf{v}_j^{n+1} = \boldsymbol{\pi}(\mathbf{v}_p^{n+1})$
5. Find the pressure value solving the Poisson equation system using FEM:
   $\rho \nabla \cdot \hat{\mathbf{v}}_j^{n+1} = \frac{\Delta t}{2} \Delta[\delta p^{n+1}]$
6. Update the velocity value with the new pressure:
   $\rho \mathbf{v}_j^{n+1} = \rho \hat{\mathbf{v}}_j^{n+1} - \frac{\Delta t}{2}(\nabla p^{n+1} - \nabla p^n)$
   $\rho \mathbf{v}_p^{n+1} = \rho \hat{\mathbf{v}}_p^{n+1} - \frac{\Delta t}{2} \boldsymbol{\pi}^{-1}(\nabla p^{n+1} - \nabla p^n)$

2 THERMAL COUPLING. MATHEMATICAL FORMULATION

The goal is to solve the Navier-Stokes equation system (2 - 3) coupled with the heat equation (1). The coupling is achieved through the Boussinesq approximation that adds a buoyancy body force in the momentum equation to relate density changes to temperature. It states that density differences are sufficiently small to be neglected, except where they appear in terms multiplied by the acceleration due to gravity g. The essence of the Boussinesq approximation is that the difference in inertia is negligible but gravity is sufficiently strong to make the specific weight significantly different along the domain. Using a constant density formulation (incompressible flow) sound waves are filtered when the Boussinesq approximation is used since sound waves move via density variations. The motion driven by physically density variations is replaced by a buoyancy term acting with the gravity.

Boussinesq approximation can be written as equation 8 (Arpaci and Larsen, 1984)

$$\mathbf{f} = \mathbf{g}\beta(\phi - \phi_c) \tag{8}$$

where $\mathbf{v}$ is the velocity, ϕ is the temperature, p the pressure, ρ the fluid density, $\mathbf{g}$ the gravitational constant, β the thermal expansion coefficient and ϕ_c is a reference temperature.

In PFEM-2 taking advantage of that particles can transport physics variables that any model includes, and having implemented successfully Navier-Stokes and heat problems separately, it is not difficult to update the method to solve the thermal coupling. The explicit streamline integration strategy used by the method allows to update the temperature and the velocity (including the Boussinesq approximation) and performing the temporal integration only once.

Finally, the Algorithm 3 is used.

Algorithm 3 - Time Step PFEM-2 Thermal Coupling

1. Calculate acceleration and thermal changes rate on the nodes like a FEM:
   $\int_\Omega \boldsymbol{N}\ \nabla\cdot\boldsymbol{\tau}^n\ d\Omega = -\int_\Omega \nabla\boldsymbol{N}\cdot(\mu\nabla\mathbf{v}^n)\ d\Omega + \int_\Gamma \boldsymbol{N}\ \nabla\mathbf{v}^n\cdot\eta\ d\Gamma$
   $\int_\Omega \boldsymbol{N}\ \nabla p^n\ d\Omega = -\int_\Omega \nabla\boldsymbol{N}\ p^n\ d\Omega + \int_\Gamma \boldsymbol{N}\ p^n\cdot\eta\ d\Gamma$
   $\int_\Omega \boldsymbol{N}\ \mathbf{g}^n\ d\Omega = -\int_\Omega \nabla\boldsymbol{N}\ \alpha\nabla\phi^n\ d\Omega + \int_\Gamma \boldsymbol{N}\ \nabla\phi^n\cdot\eta\ d\Gamma$
   $\mathbf{a}^n = \nabla\cdot\sigma^n = -\nabla p^n + \nabla\cdot\boldsymbol{\tau}^n$
2. Evaluate new particles position and state following the streamlines:
   $\mathbf{x}_p^{n+1} = \mathbf{x}_p^n + \int_0^{\Delta t}\mathbf{v}^n(\mathbf{x}_p^\tau)\ d\tau$
   $\hat{\mathbf{v}}_p^{n+1} = \mathbf{v}_p^n + \int_0^{\Delta t}\mathbf{a}^n(\mathbf{x}_p^{n+\tau}) + \mathbf{f}^{n+\tau} + \mathbf{g}\beta(\phi^n-\phi_c)d\tau$
   $\phi_p^{n+1} = \phi_p^n + \int_0^{\Delta t}\mathbf{g}^n(\mathbf{x}_p^{n+\tau}) + Q^{n+\tau}\ d\tau$
3. Update particles inventory
4. Project state to the mesh:
   $\mathbf{v}_j^{n+1} = \boldsymbol{\pi}(\mathbf{v}_p^{n+1})$
   $\phi_j^{n+1} = \boldsymbol{\pi}(\phi_p^{n+1})$
5. Find the pressure value solving the Poisson equation system using FEM:
   $\rho\nabla\cdot\hat{\mathbf{v}}_j^{n+1} = \frac{\Delta t}{2}\Delta[\delta p^{n+1}]$
6. Update the velocity value with the new pressure:
   $\rho\mathbf{v}_j^{n+1} = \rho\hat{\mathbf{v}}_j^{n+1} - \frac{\Delta t}{2}(\nabla p^{n+1} - \nabla p^n)$
   $\rho\mathbf{v}_p^{n+1} = \rho\hat{\mathbf{v}}_p^{n+1} - \frac{\Delta t}{2}\boldsymbol{\pi}^{-1}(\nabla p^{n+1} - \nabla p^n)$

3 TESTS

Natural convection in closed cavities (where the temperature difference induces momentum) is of great importance in many engineering and scientific applications such as energy transfer, boilers, nuclear reactor systems, energy storage devices among others. Related to natural convection in closed cavities in laminar regimes, there are significant benchmark problems of numerical solution, in both two and three dimensions. This paper presents results for four values of Rayleigh number, namely 10^3, 10^4, 10^5 and 10^6, with a Prandtl number of $Pr = \nu/\alpha = 0.71$ where ν is the kinematic viscosity.

3.1 Natural convection in a square cavity

The problem presented deals with the two dimensional flow with a Prandtl number $Pr = 0.71$ in a square cavity of side $H = 1[m]$. The boundary conditions for the momentum equation are non slip at all boundaries. Horizontal walls are isolated, and the vertical sides are at different temperatures $T_c < T < T_h$ ($\phi = T$ for natural convection problems). Figure 2 shows the

geometry of the cavity. Simulations were carried out using a mesh of triangular elements with 100x100 nodes and refinement towards the walls. The wide range of Rayleigh number 9 (Ra) was obtained by a constant temperature difference of $\Delta T = 1K$ adjusting the thermal expansion coefficient β to supply the desired Ra.

$$Ra = \frac{g\beta H^3(\phi_h - \phi_c)}{\alpha\nu} \tag{9}$$

where α is the thermal diffusivity corresponding to air with the above mentioned Pr in standard temperature and pressure conditions.

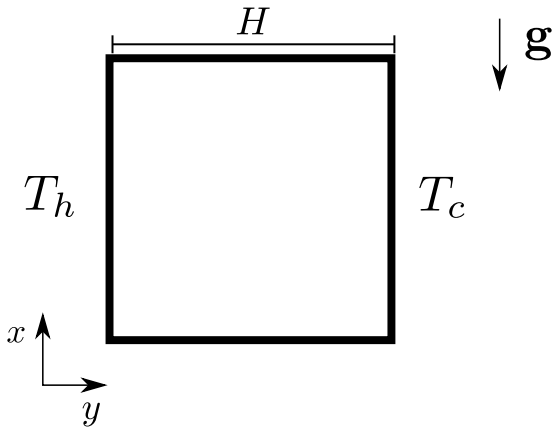

Figure 2: Detail of cavity simulated, left wall at T_h, right wall at T_c, top and bottom walls are insulated.

3.1.1 Results and discussion

This section provides a set of solutions at low Ra number. The quantities under study are the following:

$[u_{max}(1/2)]$: The maximum horizontal velocity on the vertical mid-plane of the cavity (together with its location).

$[v_{max}(1/2)]$: The maximum vertical velocity on the horizontal mid-plane of the cavity (together with its location).

Table 1 shows PFEM-2 results for $Ra = 10^3$, 10^4 and 10^6 compared with the (Corzo et al., 2011) and (Davis, 1983) solutions. Excellent agreement to experimental data in both results for momentum and energy equations prove the accuracy of this approach for this low Ra number range. The horizontal velocity component in the vertical mid-plane is shown in figure 3. Here is worthy to note that when Ra number increases the boundary layer becomes thinner and the maximum values in the velocity get closer to the walls. Finally figure 4 presents the temperature profiles for the three cases.

Ra	Data	PFEM2	Corzo	G. V. Davis
10^3	umax (x=0.5)	3.605	3.640	3.634
10^3	ymax (x=0.5)	0.814	0.812	0.813
10^3	vmax (y=0.5)	3.650	3.700	3.679
10^3	xmax (y=0.5)	0.183	0.177	0.179
10^4	umax (x=0.5)	15.982	16.281	16.182
10^4	ymax (x=0.5)	0.824	0.822	0.823
10^4	vmax (y=0.5)	19.378	19.547	19.509
10^4	xmax (y=0.5)	0.116	0.123	0.120
10^6	umax (x=0.5)	64.483	64.558	65.330
10^6	ymax (x=0.5)	0.845	0.851	0.851
10^6	vmax (y=0.5)	218.054	221.572	216.750
10^6	xmax (y=0.5)	0.037	0.067	0.039

Table 1: Numerical solution for thermal square cavity with PFEM-2 comparing with reference data.

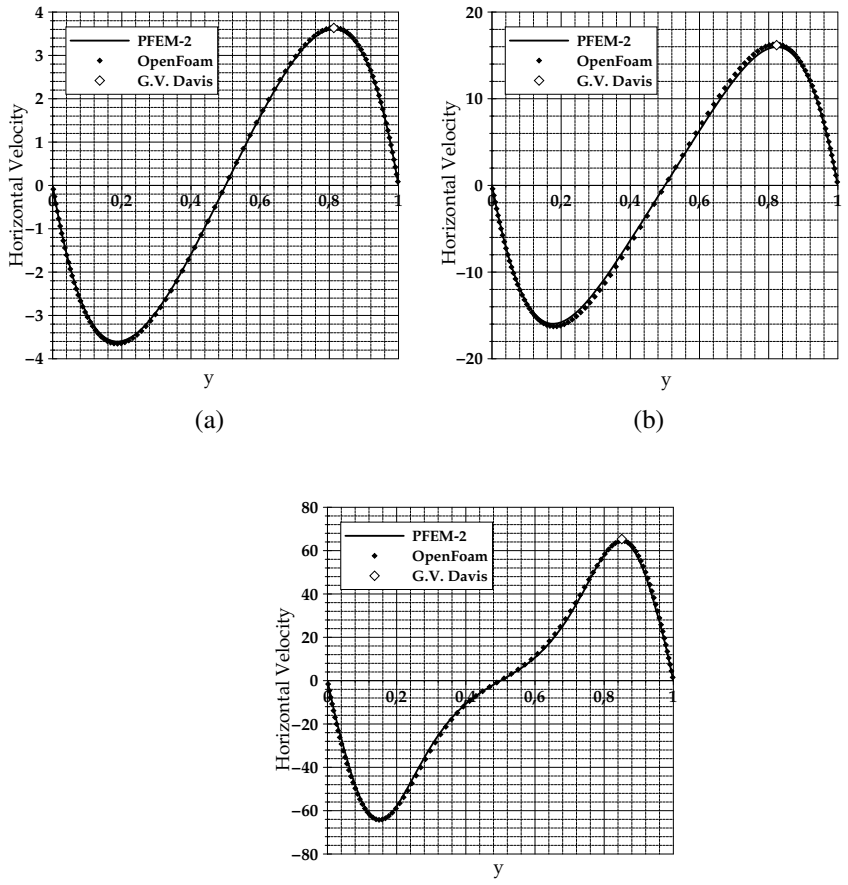

Figure 3: Horizontal velocity profiles at x mid-plane to a) $Ra = 10^3$, b) $Ra = 10^4$ and c) $Ra = 10^6$.

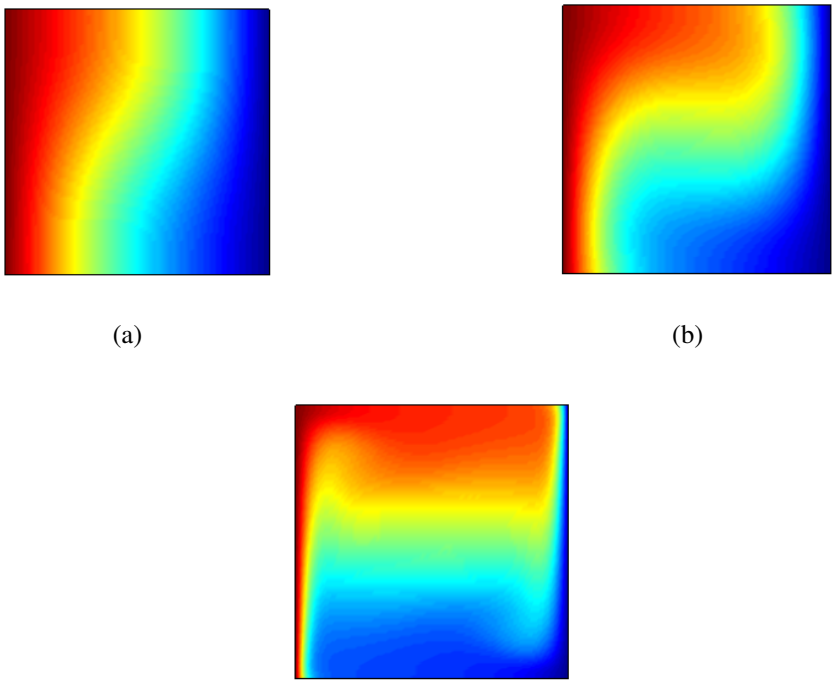

(a) (b)

(c)

Figure 4: Temperature field ϕ to a) $Ra = 10^3$, b) $Ra = 10^4$ and c) $Ra = 10^6$.

3.2 Natural Convection in a Cubic Cavity

The schematic model for the problem is shown in figure (5). The cubic cavity is one meter length with an aspect ratio of unity and is filled with air as working fluid. The Prandtl number is fixed at $Pr = 0.71$. All surrounding walls are rigid and impermeable. The vertical walls located at $x = 0$ and $x = 1$ are retained to be isothermal but at different temperatures of T_h and T_c, respectively. The buoyancy force due to gravity works downwards (i.e., in negative z-direction).

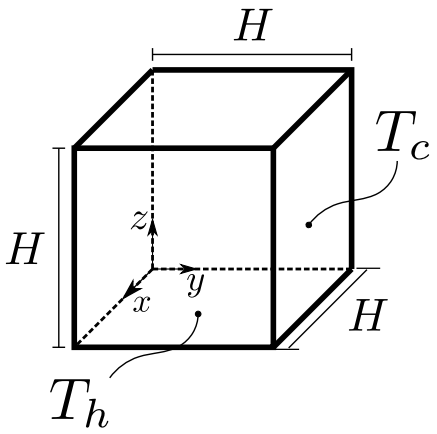

Figure 5: Schematic model for the natural convection in a cubical cavity.

3.2.1 Results and Discussion

For the present range of Ra numbers, solutions were obtained on a mesh with 81000 tetrahedral elements and around of eighteen thousand nodes, and with refinement towards the walls. The following characteristic quantities are presented:

$[u_{max}(1/2)]$: The maximum horizontal velocity for x-direction on center line (x = 0.5, y = 0.5) of the cavity and its location.

$[w_{max}(1/2)]$: The maximum vertical velocity for z-direction on center line (y = 0.5, z = 0.5) of the cavity and its location.

Table 2 shows PFEM-2 results for $Ra = 10^4$, 10^5 and 10^6 compared with the Wakashima and Saitoh (2004) and Fusegi et al. (1991) solutions. Finally figure 6 shows a wireframe of the mesh used and temperature profiles (left: $Ra = 10^4$, rigth: $Ra = 10^4$) with slices of section at mid-planes $y = 0.5$ and $z = 0.5$ respectively.

Ra	Data	PFEM-2	Wakashima	Fusegi
10^4	$u_{max}(x = y = 0.5)$	0.1978	0.1989	0.2013
10^4	$z_{max}(x = y = 0.5)$	0.8460	0.8250	0.8167
10^4	$w_{max}(y = z = 0.5)$	0.2190	0.2211	0.2252
10^4	$x_{max}(y = z = 0.5)$	0.1260	0.1253	0.1167
10^5	$u_{max}(x = y = 0.5)$	0.1409	0.1423	0.1468
10^5	$z_{max}(x = y = 0.5)$	0.8460	0.8500	0.8547
10^5	$w_{max}(y = z = 0.5)$	0.2359	0.2407	0.2471
10^5	$x_{max}(y = z = 0.5)$	0.0680	0.0751	0.0647
10^6	$u_{max}(x = y = 0.5)$	0.0766	0.0813	0.0842
10^6	$z_{max}(x = y = 0.5)$	0.8570	0.8500	0.8557
10^6	$w_{max}(y = z = 0.5)$	0.2897	0.2382	0.2588
10^6	$x_{max}(y = z = 0.5)$	0.0280	0.0500	0.0331

Table 2: Numerical solution for thermal cubic cavity with PFEM-2 comparing with reference data.

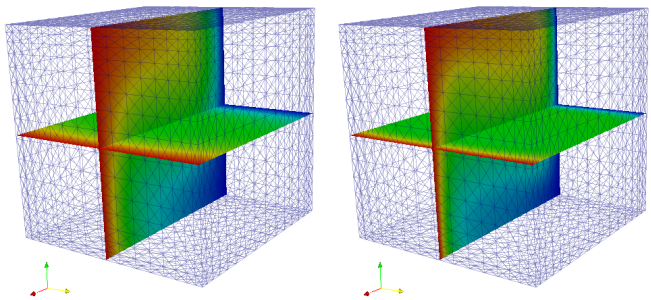

Figure 6: Mesh with slices of section at mid-planes $y = 0.5$ and $z = 0.5$. Left: $Ra = 10^4$, rigth: $Ra = 10^4$.

4 CONCLUSIONS

The results achieved with PFEM-2 presented in this paper reveal a good agreement with reference data not only in 2D (two dimensions) also in 3D (three dimensions) and for a range of low and medium Ra numbers. In this sense they can be set as a reference for a future buoyancy-driven tests. Higher Ra numbers than those presented in this paper require turbulence modeling or a finer mesh to capture effects in smaller scales.

The presented method can be improved including an implicit treatment of the thermal and the viscous diffusivity. This strategy allows to increase the time-step and, in this way, be more competitive in computing times with other CFD (computational fluid dynamics) methods.

Finally, we prove that it is possible to solve the weak coupling between energy and momentum equations with PFEM-2 through the Boussinesq approximation. This achievement allows to use this strategy to solve several passive scalar transport species and also some active ones, such as turbulence modeling, in an efficient way.

5 ACKNOWLEDGMENTS

The authors want to thank CONICET, Universidad Nacional del Litoral (CAI+D Tipo II 65-333 (2009)) and ANPCyT-FONCyT (grants PICT 1645 BID (2008)) for their financial support.

REFERENCES

Arpaci V. and Larsen P. *Convection Heat Transfer*. Prentice Hall, 1984. ISBN 9780131723467.

Corzo S., Márquez Damián S., Ramajo D., and Nigro N. Numerical simulation of natural convection phenomena. *ENIEF*, XXX, 2011.

Davis G.D.V. Natural convection of air in a square cavity: a benchmark numerical solution. *International Journal for Numerical Methods in Fluids*, 3:249–264, 1983.

Donea J. and Huerta A. *Finite element method for flow problems*. Springer-Verlag., 1st edition, 2003.

Fusegi T., Hyun J., Kuwahara K., and Farouk B. A numerical study of three-dimensional natural convection in a differentially heated cubical enclosure. *International Journal of Heat and Mass Transfer*, 34(6):1543 – 1557, 1991.

Idelsohn S., Nigro N., Limache A., and Oñate E. Large time-step explicit integration method for solving problems with dominant convection. *Computer Methods in Applied Mechanics and Engineering*, (submitted), 2011.

Idelsohn S., Nigro N., Limache A., and Oñate. E. Large time-step explicit integration method for solving problems with dominant convection. *Comp. Meth. in Applied Mechanics and Engineering*, 217-220:168–185, 2012.

Wakashima S. and Saitoh T. Benchmark solutions for natural convection in a cubic cavity using the high-order time-space method. *International Journal of Heat and Mass Transfer*, 47:853–864, 2004.